

Oxidation of a Dimeric Nickel Thiolate Complex with O<sub>2</sub>

Shaikat A. Mirza, Roberta O. Day, and Michael J. Maroney\*

Department of Chemistry, University of Massachusetts, Amherst, Massachusetts 01003-4510

Received June 15, 1995<sup>⊗</sup>

Reaction of dimeric bis{[μ-(2-mercaptoethyl)(2-mercaptoethyl)methylamino(2-)]nickel(II)}, **1**, with either O<sub>2</sub> or H<sub>2</sub>O<sub>2</sub> leads to the formation of a dimeric product, bis{[μ-(2-mercaptoethyl)(2-sulfinatoethyl)methylamino(2-)]nickel(II)}, **2**. The reaction is first-order in [Ni] and proceeds at a very slow rate at 40 °C (*t*<sub>1/2</sub> = 7.8 days; *k* = 1.0(1) × 10<sup>-6</sup> s<sup>-1</sup>) under 1 atm of O<sub>2</sub>. Crystals of **2** form in the orthorhombic space group *Pbca* with cell dimensions *a* = 14.271(2) Å, *b* = 20.424(3) Å, *c* = 11.766(2) Å, *V* = 3429.4(9) Å<sup>3</sup>, and *Z* = 8. A single-crystal X-ray diffraction study of these crystals reveals a dimeric structure that is quite similar to **1**, where the terminal thiolates have been oxidized to sulfinate ligands in **2**. Compound **1** has several structural features in common with the dimeric μ-dithiolato Ni,Fe site found in the active site of *Desulfovibrio gigas* hydrogenase. The structural similarities and the potential relevance of the oxidation reaction are discussed.

Several examples of the reaction of Ni thiolate complexes with O<sub>2</sub> leading to the formation of sulfinate complexes have now been characterized. These include planar *trans*-<sup>1,2</sup> and *cis*-dithiolato<sup>3,4</sup> complexes and a bis(dithiolene) complex.<sup>5</sup> The reaction is novel in that it involves the incorporation of both atoms of O<sub>2</sub> into the product (*i.e.*, a dioxygenase-like mechanism), in contrast to the more familiar reaction of metal thiolate complexes with O<sub>2</sub><sup>2-</sup>, which leads to the sequential oxidation of the thiolates to sulfenates, sulfinates, and sulfonates.<sup>6–8</sup> We report here the first example of the oxidation of a dimeric Ni thiolate complex by O<sub>2</sub>. The reaction of metal thiolate complexes with O<sub>2</sub> is of general interest to the oxidative deactivation of metallothionein enzymes and to the oxidative metabolism of cysteine.<sup>2</sup> The reaction of the dimeric Ni thiolate complex presented here is of particular interest with respect to the recently reported structure of *Desulfovibrio gigas* hydrogenase,<sup>9</sup> which features an M<sub>2</sub>S<sub>2</sub> core composed of one Ni and one Fe center.

## Experimental Section

The starting dimeric complex, bis{[μ-(2-mercaptoethyl)(2-mercaptoethyl)methylamino(2-)]nickel(II)}, **1**, was prepared as previously described.<sup>2</sup> Reaction of **1** (215 mg, 0.517 mmol) with O<sub>2</sub> in DMF (25 mL) led to the conversion of the starting material to the oxidation product bis{[μ-(2-mercaptoethyl)(2-sulfinatoethyl)methylamino(2-)]nickel(II)}, **2**.

After 500 h, at 40 °C, the reaction was ~80% complete. The product was separated from unreacted starting material by column chromatography. A column was prepared with silica gel (60–200 mesh, Baker) and hexane. A step gradient was produced by increasing the volume percent of EtOH in the eluent by 10% every 100 mL. The starting material (**1**), a red-brown band, is eluted at ~20% EtOH. The red-orange product (**2**) is eluted with pure EtOH. No other compounds were present. The fraction containing **2** was concentrated by using a rotary evaporator from *ca.* 700 to 250 mL. After the sample was allowed to stand in a freezer, crystals of **2** formed and were isolated by filtration, washed with cold EtOH, and dried in vacuo. A second crop was obtained by concentrating the filtrate. Total yield = 0.16 g (64%, or 80% of the reacted starting material).

The bis(disulfinate) (**2**) may also be produced by oxidation of **1** with H<sub>2</sub>O<sub>2</sub>, which is not as clean but has the advantage of being a much faster reaction. Following a procedure using a stoichiometric amount of H<sub>2</sub>O<sub>2</sub>, **1** (475 mg, 1.14 mmol) was dissolved in MeOH (80 mL) under N<sub>2</sub>, and the solution was chilled in an ice bath. The H<sub>2</sub>O<sub>2</sub> (30% aqueous solution) was added in aliquots until 4 equiv had been added. The reaction mixture was then allowed to warm to room temperature and stir for 2 days. The products were separated by column chromatography on a silica gel (60–200 mesh, Baker) prepared with benzene. The products were separated by elution with a step gradient of MeOH. Unreacted **1** was eluted with 10% MeOH, and **2** was eluted with 20% MeOH. A light green solid was retained on the column. After removal of the solvent, 210 mg of **2** was obtained (38%).

Crystals of **2** used for the X-ray diffraction structural determination were obtained from H<sub>2</sub>O<sub>2</sub> oxidation and crystallized from EtOH. The opaque, very thin rectangular plate used for the study had approximate dimensions of 0.044 × 0.25 × 0.50 mm. The crystal was mounted inside of a thin-walled glass capillary tube, which was then sealed as a precaution against air/moisture sensitivity. The X-ray crystallographic studies were done using an Enraf-Nonius CAD4 diffractometer and graphite-monochromated molybdenum radiation. Details of the experimental procedures have been described previously.<sup>10</sup>

Crystals of **2** diffract poorly (reasonable peak widths but rapid falloff of intensity with scattering angle). Data were collected using the θ–2θ scan mode with 3° ≤ 2θ<sub>MoKα</sub> ≤ 43°. A total of 1958 independent reflections (+*h*, +*k*, +*l*) were measured. An empirical absorption correction based on ψ scans was applied (relative transmission factors from 0.639 to 1.00 on *I*).

The structure was solved by use of direct methods and difference Fourier techniques and was refined by full-matrix least-squares. Refinement was based on *F*<sup>2</sup>, and computations were performed on a

<sup>⊗</sup> Abstract published in *Advance ACS Abstracts*, March 1, 1996.

- (1) Kumar, M.; Colpas, G. J.; Day, R. O.; Maroney, M. J. *J. Am. Chem. Soc.* **1989**, *111*, 8323–5.
- (2) Mirza, S. A.; Pressler, M. A.; Kumar, M.; Day, R. O.; Maroney, M. J. *Inorg. Chem.* **1993**, *32*, 977–87.
- (3) Farmer, P. J.; Solouki, T.; Mills, D. K.; Soma, T.; Russell, D. H.; Reibenspies, J. H.; Darensbourg, M. Y. *J. Am. Chem. Soc.* **1992**, *114*, 4601–5.
- (4) Darensbourg, M. Y.; Farmer, P. J.; Soma, T.; Russell, D. H.; Solouki, T.; Reibenspies, J. H. *Act. Dioxygen Homogeneous Catal. Oxid. [Proc. Int. Symp.]*, 5th **1993**, 209–23.
- (5) Schrauzer, G. N.; Zhang, C.; Chadha, R. *Inorg. Chem.* **1990**, *29*, 4104–7.
- (6) Deutsch, E.; Root, M. J.; Nosco, D. L. *Adv. Inorg. Bioinorg. Mech.* **1982**, *1*, 269.
- (7) Font, I.; Buonomo, R.; Reibenspies, J. H.; Darensbourg, M. Y. *Inorg. Chem.* **1993**, *32*, 5897–8.
- (8) Buonomo, R. M.; Font, I.; Maguire, M. J.; Reibenspies, J. H.; Tuntulani, T.; Darensbourg, M. Y. *J. Am. Chem. Soc.* **1995**, *117*, 963–73.
- (9) Volbeda, A.; Charon, M.-H.; Piras, C.; Hatchikian, E. C.; Frey, M.; Fontecilla-Camps, J. C. *Nature* **1995**, *373*, 580–7.

- (10) Sau, A. C.; Day, R. O.; Holmes, R. R. *Inorg. Chem.* **1981**, *20*, 3076–81.

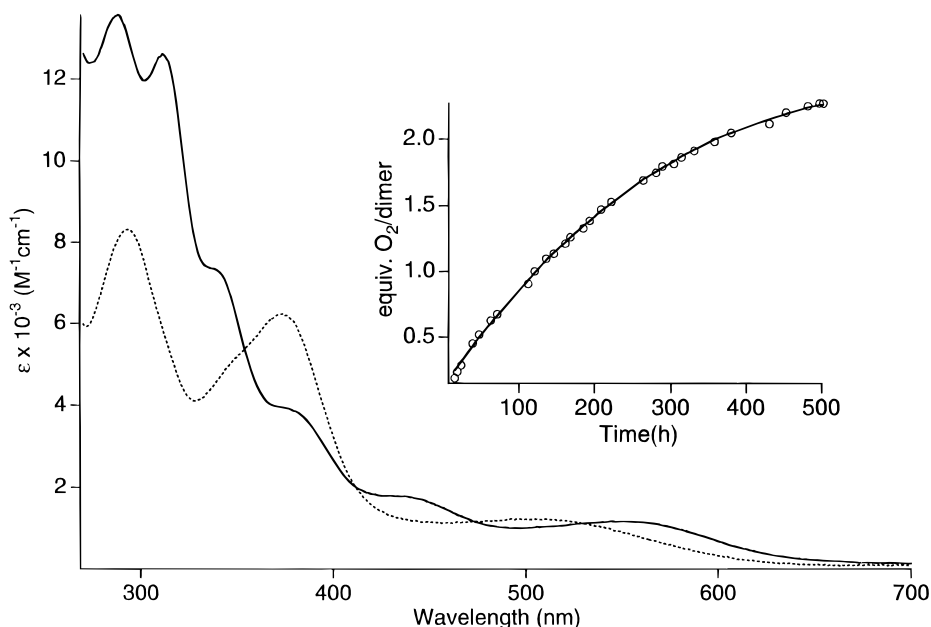


**Figure 1.** Electronic absorption spectra of **1** (solid line) and **2** (dashed line). The inset shows the manometric O<sub>2</sub> uptake data (open circles) and a single exponential fit (solid line).

486/66 computer using SHELXS-86 for solution<sup>11</sup> and SHELXL-93 for refinement.<sup>12</sup>

There is disorder in the structure due to the cocrystallization of two isomers which have different configurations at atom N(1). This disorder was modeled with two sets of positions for atoms C(2), C(4), and C(5). Refinement indicated 30% occupancy for the alternate set of positions (C(2A), C(4A), and C(5A)) and 70% occupancy for the major isomer (C(2), C(4), and C(5)). The disordered carbon atoms were refined isotropically while the remaining independent non-hydrogen atoms were refined anisotropically. Hydrogen atoms with positions which are affected by the disorder (those bonded to carbon atoms C(1) through C(5)) were omitted from the refinement. The remaining hydrogen atoms were included in the refinement as isotropic scatterers riding in ideal positions on the bonded carbon atoms. All of the data were included in the refinement. The final agreement factors are based on the 1420 reflections with  $I \geq 2\sigma$ .

Crystallographic data are summarized in Table 1.

Electronic absorption spectra were obtained by using an OLIS 4300 Cary-14 system. Infrared spectra were obtained as KBr pellets on a Perkin-Elmer 783 IR spectrophotometer and calibrated with polystyrene. Oxygen uptake measurements were made by using an apparatus similar to the one described by Chen and Martell,<sup>13</sup> which was equipped with a circulating water bath in order to maintain the temperature at  $40.0 \pm 0.5$  °C for 3 weeks.

Microanalyses were performed by the University of Massachusetts Microanalysis Laboratory.

## Results and Discussion

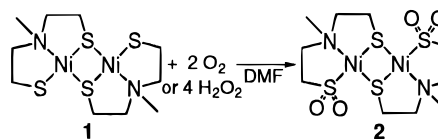
Oxidation of **1** with O<sub>2</sub> or with H<sub>2</sub>O<sub>2</sub> leads to the formation of **2**, where both terminal thiolates have been oxidized to sulfinate without altering the bridging thiolates in the Ni<sub>2</sub>S<sub>2</sub> core (Scheme 1). The red-orange oxidation product, **2**, has a UV-vis spectrum that is quite distinct from the spectrum observed for **1** (Figure 1) and features absorption maxima at 502 nm ( $\epsilon = 1210 \text{ M}^{-1} \text{ cm}^{-1}$ ), 374 nm ( $\epsilon = 6240 \text{ M}^{-1} \text{ cm}^{-1}$ ), and 293 nm ( $\epsilon = 8320 \text{ M}^{-1} \text{ cm}^{-1}$ ). The last two transitions are characteristic of all planar Ni sulfinate complexes and can be attributed to LMCT transitions arising from the sulfinate

**Table 1.** Crystallographic Data for Compound **2**

formula	C <sub>10</sub> H <sub>22</sub> O <sub>4</sub> S <sub>4</sub> N <sub>2</sub> Ni <sub>2</sub>	fw	479.96
crystal system	orthorhombic	V (Å <sup>3</sup> )	3429.4(9)
space group	Pbca (No. 61)	Z	8
a (Å)	14.271(2)	T (°C)	23 ± 2
b (Å)	20.424(3)	λ (Å)	0.71073
c (Å)	11.766(2)	D <sub>calc</sub> (g/cm <sup>3</sup> )	1.859
α (deg)	90	μ <sub>MoKα</sub> (cm <sup>-1</sup> )	2.698
β (deg)	90	R <sup>a</sup>	0.0562
γ (deg)	90	R <sub>w</sub> <sup>b</sup>	0.1427

$$^a R(F_o) = \frac{\sum ||F_o| - |F_c||}{\sum |F_o|}, \quad ^b R_w(F_o^2) = \frac{\{\sum w(F_o^2 - F_c^2)^2\}^{1/2}}{\sum w F_o^4}.$$

## Scheme 1



group.<sup>2,14</sup> For the monomeric CN<sup>-</sup> complex derived from **1**, [(2-mercaptoethyl)(2-sulfinatoethyl)methylamino(2-)]nickelate(II), the corresponding electronic transitions are observed at 325 nm ( $\epsilon = 11\,100 \text{ M}^{-1} \text{ cm}^{-1}$ ) and 264 nm ( $\epsilon = 15\,100 \text{ M}^{-1} \text{ cm}^{-1}$ ) in CH<sub>3</sub>CN.<sup>2</sup> The lowest energy transition at 502 nm is likely to be largely a d<sub>xy</sub> → d<sub>x<sup>2</sup>-y<sup>2</sup></sub> transition on the basis of calculations of similar planar monosulfinato complexes.<sup>14</sup> The IR spectrum of **2** reveals strong bands at 1053 and 1181 cm<sup>-1</sup> that can be assigned to ν<sub>s</sub> and ν<sub>a</sub>, respectively, of an S-bound sulfinate ligand.<sup>2</sup>

The kinetics of the O<sub>2</sub> oxidation (Figure 1) are first-order under conditions of excess O<sub>2</sub>, indicating that the oxidation of each of the two thiolates is independent of the other. The pseudo-first-order rate constant for the oxidation can be estimated from the manometric data and reveals an exceedingly slow reaction ( $k = 1.0(1) \times 10^{-6} \text{ s}^{-1}$ ) at 40 °C with a half-life of 188 h (7.8 days). The reaction was followed for 2.7 half-lives (three weeks), at which point the reaction was >80% complete. Extrapolation of the data to complete oxidation reveals that 2.3 equiv of O<sub>2</sub> is consumed per mol of dimer in

(11) Sheldrick, G. M. *Acta Crystallogr.* **1990**, A46, 467–73.

(12) Sheldrick, G. M. *J. Appl. Crystallogr.*, in press.

(13) Chen, D.; Martell, A. E. *Inorg. Chem.* **1987**, 26, 1026–30.

(14) Maroney, M. J.; Choudhury, S. B.; Bryngelson, P. A.; Mirza, S. A.; Sherrod, M. J. A Theoretical Study of the Oxidation of Nickel Thiolate Complexes by O<sub>2</sub>. *Inorg. Chem.* **1996**, 35, 1073–1076.

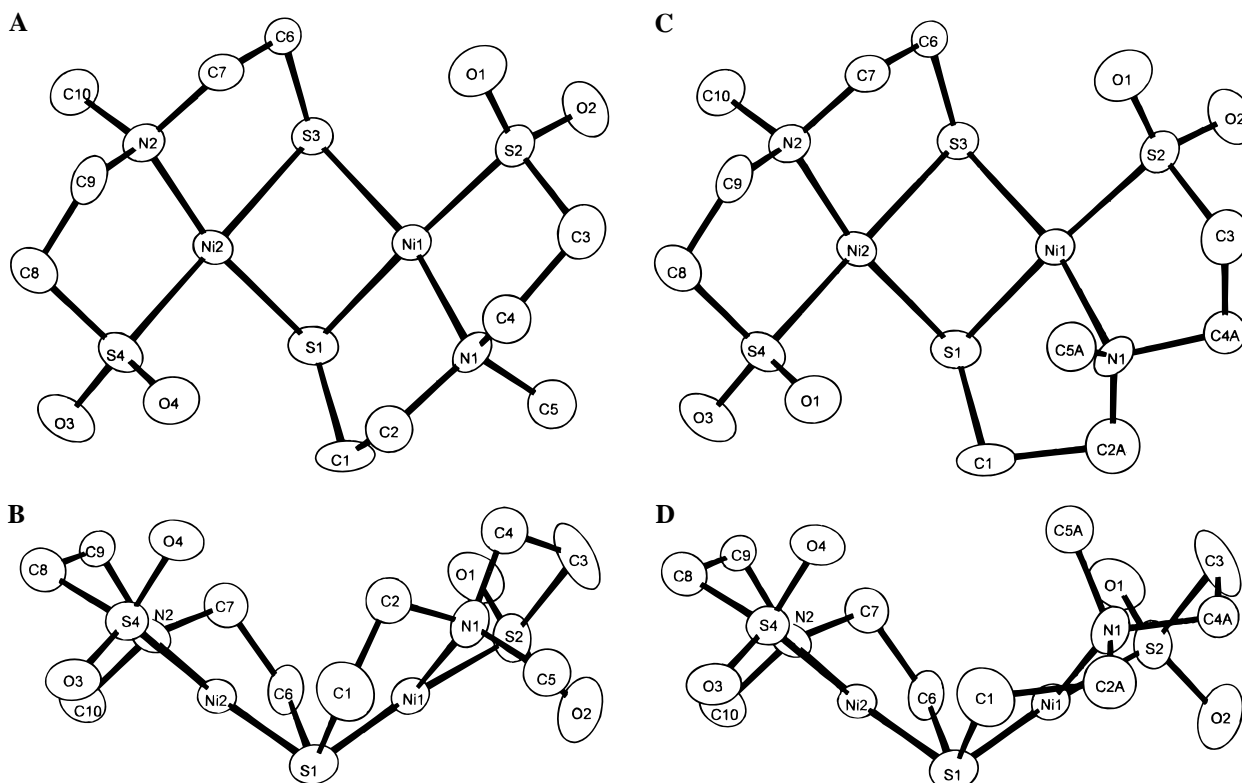


**Figure 2.** SNOOPI plot of **2**: (A) top view (approximately normal to the plane defined by the Ni(1)–Ni(2) and S(1)–S(3) vectors) of the major isomer; (B) side view (along S(1)–S(3)) of the major isomer; (C) top view of the minor isomer; (D) side view of the minor isomer.

the exhaustive oxidation of **1**. A rate constant obtained from monitoring the UV–visible spectrum for 0.8 half-life ( $2.03(5) \times 10^{-6} \text{ s}^{-1}$ ) is in good agreement with the value obtained by manometry. The rate of oxidation of **2** may be compared with the pseudo-first-order rate constant of  $1.93(1) \times 10^{-4} \text{ s}^{-1}$  ( $t_{1/2} = 1.00 \text{ h}$ ) at  $40^\circ \text{C}$  for the  $\text{O}_2$  oxidation of the anionic, monomeric *trans*-dithiolate complex obtained by the addition of  $\text{CN}^-$  to **1**.<sup>2</sup> The difference in rate probably reflects in large part a difference in the nucleophilicity of the terminal thiolates between anionic and neutral complexes, a notion that is supported by theory.<sup>14</sup>

The observation of first-order kinetics is a surprising result. Under pseudo-first-order conditions in  $[\text{O}_2]$ , this might be expected if the rate-determining step were the oxidation of the first thiolate and the second oxidation was relatively fast. However, such a situation is inconsistent with the studies of the mononuclear systems, which demonstrate that only one thiolate in dithiolato complexes can be oxidized under these conditions.<sup>2</sup> If the rate of oxidation of the second thiolate were slower than the first oxidation, then biphasic kinetics would be observed. Thus, assuming that the dimer is the reactive species, the first-order kinetics indicate that the rates of reaction of the two thiolates are the same. This could arise if the terminal thiolates in the dimer are electronically isolated. On the other hand, the equivalency of the two thiolates could also arise from a dimer–monomer equilibrium involving a very small amount (*i.e.*, undetectable by UV–vis spectroscopy) of a monomeric solvato complex that would undergo oxidation in analogy with the known oxidation of the  $\text{CN}^-$  adduct of **1**.<sup>2</sup> However, it is difficult to reconcile a mechanism involving such a pre-equilibrium step with the observed first-order kinetics in [dimer] that are observed by monitoring changes in the UV–visible spectrum. Thus, the kinetics and stoichiometry of the reaction support a mechanism involving the oxidation of the dimer by  $\text{O}_2$ . The presence of monosulfinato intermediates implicit in either mechanism cannot be detected by UV–visible spectroscopy.

**Table 2.** Atomic Coordinates ( $\times 10^4$ ) and Equivalent Isotropic Displacement Parameters ( $\text{\AA}^2 \times 10^3$ ) for the Major Isomer in **2**<sup>a</sup>

	<i>x</i>	<i>y</i>	<i>z</i>	<i>U</i> (eq)
Ni(1)	199(1)	781(1)	3547(1)	28(1)
Ni(2)	216(1)	2013(1)	4426(1)	26(1)
S(1)	578(2)	1102(2)	5276(2)	37(1)
S(2)	−191(2)	396(1)	1928(3)	38(1)
S(3)	−998(2)	1413(1)	3874(2)	30(1)
S(4)	1424(2)	2588(2)	4839(2)	34(1)
O(1)	−420(6)	865(4)	1037(7)	56(3)
O(2)	−870(6)	−136(4)	2033(8)	64(3)
O(3)	1583(5)	2711(4)	6048(6)	48(2)
O(4)	2249(5)	2367(4)	4213(7)	47(2)
N(1)	1439(6)	389(4)	3367(9)	36(2)
N(2)	−233(6)	2721(4)	3466(7)	29(2)
C(1)	1830(8)	889(7)	5224(12)	54(4)
C(2)	2143(12)	842(9)	4029(15)	43(4)
C(3)	925(10)	24(8)	1482(12)	65(4)
C(4)	1724(12)	412(9)	2151(15)	45(5)
C(5)	1561(12)	−284(9)	3820(16)	47(5)
C(6)	−1337(7)	1901(5)	2650(10)	35(3)
C(7)	−589(8)	2405(6)	2389(10)	35(3)
C(8)	1088(8)	3352(6)	4196(10)	41(3)
C(9)	535(8)	3184(5)	3161(9)	33(3)
C(10)	−994(8)	3094(6)	4014(11)	42(3)

<sup>a</sup> Estimated standard deviations in parentheses. *U*(eq) is defined as one-third of the trace of the orthogonalized  $\mathbf{U}_{ij}$  tensor.

copy, presumably since all sulfinato complexes have similar spectra (*vide supra*). The observation that the oxidation of the terminal thiolates occurs in preference to the bridging thiolates in the dimer is in agreement with the expectation that the terminal thiolates are more nucleophilic than the bridging thiolates.

The structure of **2** consists of a dinickel cluster as shown in Figure 2. Selected atomic coordinates and distances and angles are listed in Tables 2 and 3, respectively. In the solid state, **2** consists of two isomers having different configurations at N(1), which have cocrystallized in a 7:3 ratio in such a way that only

**Table 3.** Selected Distances (Å) and Angles (deg) for **2**<sup>a</sup>

Distances			
Ni(1)–Ni(2)	2.720(2)	S(4)–O(4)	1.459(8)
Ni(1)–N(1)	1.954(9)	S(4)–O(3)	1.462(8)
Ni(1)–S(2)	2.134(3)	S(4)–C(8)	1.800(12)
Ni(1)–S(3)	2.176(3)	N(1)–C(5)	1.49(2)
Ni(1)–S(1)	2.205(3)	N(1)–C(4)	1.49(2)
Ni(2)–N(2)	1.945(9)	N(1)–C(2)	1.57(2)
Ni(2)–S(4)	2.142(3)	N(2)–C(10)	1.476(13)
Ni(2)–S(1)	2.175(3)	N(2)–C(9)	1.491(14)
Ni(2)–S(3)	2.219(3)	N(2)–C(7)	1.510(14)
S(1)–C(1)	1.840(12)	C(1)–C(2)	1.48(2)
S(2)–O(1)	1.457(9)	C(3)–C(4)	1.60(2)
S(2)–O(2)	1.461(9)	C(6)–C(7)	1.52(2)
S(2)–C(3)	1.842(13)	C(8)–C(9)	1.49(2)
S(3)–C(6)	1.815(11)	S(1)–S(3)	2.862(4)
Angles			
N(1)–Ni(1)–S(2)	89.4(3)	O(4)–S(4)–C(8)	105.7(5)
N(1)–Ni(1)–S(3)	166.7(3)	O(3)–S(4)–C(8)	107.5(6)
S(2)–Ni(1)–S(3)	99.88(12)	O(4)–S(4)–Ni(2)	111.4(4)
N(1)–Ni(1)–S(1)	89.9(3)	O(3)–S(4)–Ni(2)	116.1(3)
S(2)–Ni(1)–S(1)	175.51(13)	C(8)–S(4)–Ni(2)	99.6(4)
S(3)–Ni(1)–S(1)	81.58(12)	C(5)–N(1)–C(4)	110.0(12)
N(2)–Ni(2)–S(4)	89.4(3)	C(5)–N(1)–C(2)	107.0(11)
N(2)–Ni(2)–S(1)	169.2(3)	C(4)–N(1)–C(2)	106.4(11)
S(4)–Ni(2)–S(1)	99.98(12)	C(4)–N(1)–Ni(1)	109.8(8)
N(2)–Ni(2)–S(3)	89.0(3)	C(5)–N(1)–Ni(1)	116.5(9)
S(4)–Ni(2)–S(3)	175.95(13)	C(2)–N(1)–Ni(1)	106.5(8)
S(1)–Ni(2)–S(3)	81.29(12)	C(10)–N(2)–C(9)	108.6(8)
C(1)–S(1)–Ni(2)	114.7(5)	C(10)–N(2)–C(7)	109.8(8)
C(1)–S(1)–Ni(1)	97.9(5)	C(9)–N(2)–C(7)	108.5(8)
Ni(2)–S(1)–Ni(1)	76.79(10)	C(10)–N(2)–Ni(2)	111.8(7)
O(1)–S(2)–O(2)	113.6(6)	C(9)–N(2)–Ni(2)	111.7(6)
O(1)–S(2)–C(3)	105.0(6)	C(7)–N(2)–Ni(2)	106.3(6)
O(2)–S(2)–C(3)	106.9(6)	C(2)–C(1)–S(1)	109.9(10)
O(1)–S(2)–Ni(1)	117.3(4)	C(1)–C(2)–N(1)	108.4(13)
O(2)–S(2)–Ni(1)	111.8(4)	C(4)–C(3)–S(2)	105.8(9)
C(3)–S(2)–Ni(1)	100.4(5)	N(1)–C(4)–C(3)	105.3(12)
C(6)–S(3)–Ni(1)	113.2(4)	C(7)–C(6)–S(3)	110.3(7)
C(6)–S(3)–Ni(2)	97.9(4)	N(2)–C(7)–C(6)	110.9(9)
Ni(1)–S(3)–Ni(2)	76.49(10)	C(9)–C(8)–S(4)	106.6(8)
O(4)–S(4)–O(3)	114.8(5)	N(2)–C(9)–C(8)	109.8(9)

<sup>a</sup> Estimated standard deviations in parentheses.

the three carbon atoms bonded to N(1) have different positions. In the major isomer (Figure 2A,B), the N–Me groups of the tertiary amine donor atoms have a syn-exo configuration and the idealized molecular symmetry is C<sub>2</sub>. This is the same geometry as was observed in the structure of **1**. In the minor isomer, the N–Me groups are anti (Figure 2C,D) as was observed for the related unoxidized compound containing N–(CH<sub>2</sub>)<sub>2</sub>SMe groups in place of N–Me groups.<sup>15</sup>

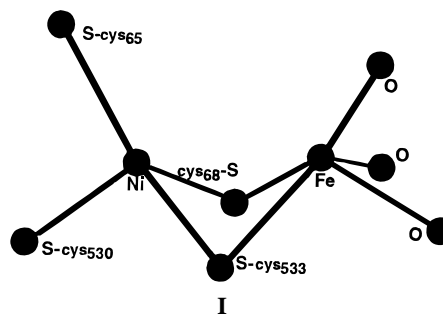
With the exception of the appearance of two isomeric forms and the presence of the oxygen atoms, the geometry of the oxidized dimer is nearly identical to that of its unoxidized precursor. The oxidation product consists of a dimer containing two distorted planar Ni(II) centers in an NS<sub>3</sub> coordination environment composed of one tertiary amine, one sulfinate, and two  $\mu$ -thiolato ligands. The atoms of the NiS<sub>3</sub>N grouping containing Ni(2) are coplanar to within  $\pm 0.046(3)$  Å, while for the analogous grouping containing Ni(1) this value is  $\pm 0.137(3)$  Å. The two planar monomeric Ni(NS<sub>2</sub>) units are joined at an edge by the two bridging thiolates in the characteristic syn-endo conformation.

The central four-membered Ni<sub>2</sub>S<sub>2</sub> rhomb is not planar and can be viewed as being folded along a line connecting S(1) and S(3). The dihedral angle formed between the planes described by the Ni and bridging S atoms (the fold angle) is

109.8(1)°, a value that is quite similar to that found in **1** (108.4(1)°) and a number of other  $\mu$ -dithiolato Ni complexes.<sup>15,16</sup> This folding brings the distance between the two Ni atoms to 2.720(2) Å. The S–S distance is 2.862(4) Å. These distances are again very similar to those found for **1** (2.679(2) and 2.899(5) Å, respectively) but slightly longer as a result of slightly larger fold and S–Ni–S angles. The rest of the Ni<sub>2</sub>S<sub>2</sub> core is described by Ni–S distances of *ca.* 2.18–2.22 Å. Each Ni center has one long (*ca.* 2.22 Å) and one short (*ca.* 2.18 Å) Ni–S bond, with the shorter of the two distances formed with the S-donor from the ligand primarily involved in coordinating to the other Ni center. This is the same pattern observed in the two aforementioned dimeric thiolate complexes.<sup>15,16</sup>

The geometry involving the terminal S-donor atoms that undergo oxidation is virtually indistinguishable in the two compounds. The Ni–N and Ni–SO<sub>2</sub>R distances are unremarkable and do not differ significantly from the distances found in other sulfinate complexes featuring five-membered chelate rings with N- and S-donor atoms.<sup>1,3</sup>

The Ni<sub>2</sub>S<sub>2</sub> cores found in **1** and **2** are also similar to the Ni<sub>2</sub>–Fe active site recently characterized for *Desulfovibrio gigas* hydrogenase (structure **I**).<sup>9</sup> This heteronuclear dimer features



a Ni–Fe distance of  $\sim 2.7$  Å and a fold angle of  $\sim 96^\circ$ . The Ni site in the enzyme is composed of two bridging thiolates (cys-68 and cys-533) and two terminal thiolates (cys-65 and cys-530). The largest difference lies in the arrangement of the S-donor atoms, which place the Ni into a distorted trigonal pyramidal site in the enzyme, with cys-533 at the apex. The Ni–S bonds in the base of the pyramid average 2.25 Å, and the apical Ni–S distance is longer at  $\sim 2.6$  Å. Although there is no evidence from the crystal structure to support the notion that the terminal Ni thiolate ligands are susceptible to oxidation, only about one-third of the enzyme in the crystals is in the appropriate form (form A) for this to be observed. Thus, the crystal structure in its present state cannot rule out thiolate oxidation in the enzyme. The ubiquity of such Ni thiolate oxidations, plus the oxidation of **1** by O<sub>2</sub> reported here, suggests that the terminal cysteine ligands in the hydrogenase Ni<sub>2</sub>Fe cluster should also be susceptible to oxidation unless they are somehow protected.

**Supporting Information Available:** Crystal data and structure refinement details (Table S(1)), atomic coordinates and equivalent isotropic displacement parameters (Table S(2)), distances and angles (Table S(3)), anisotropic thermal parameters (Table S(4)), and hydrogen coordinates and isotropic displacement parameters (Table S(5)) for **2** (9 pages). Ordering information is given on any current masthead page.

IC950736A

(15) Colpas, G. J.; Kumar, M.; Day, R. O.; Maroney, M. J. *Inorg. Chem.* **1990**, 29, 4779–88.

(16) Choudhury, S. B.; Pressler, M. A.; Mirza, S. A.; Day, R. O.; Maroney, M. J. *Inorg. Chem.* **1994**, 33, 4831–9.